ACS Catalysis

Letter

pubs.acs.org/acscatalysis

Ni_2P/SBA-15 As a Hydrodeoxygenation Catalyst with Enhanced Selectivity for the Conversion of Methyl Oleate Into *n*-Octadecane

Yongxing Yang,[†] Cristina Ochoa-Hernández,[†] Víctor A. de la Peña O'Shea,[†] Juan M. Coronado,[†] and David P. Serrano*[,†,‡]

[†]Thermochemical Processes Unit, IMDEA Energy Institute, Avenida Ramón de la Sagra,3, Parque Tecnológico de Móstoles, 28935 Madrid, Spain

[‡]Department of Chemical and Energy Technology, ESCET, Rey Juan Carlos University, c/Tulipán s/n, Móstoles, 28933 Madrid, Spain

Supporting Information

ABSTRACT: A novel hydrodeoxygenation catalytic system, Ni_2P/SBA-15, has been synthesized by temperature-programmed reduction of a nickel phosphate precursor impregnated in the mesostructured silica support. The formation of this active phase was verified by X-ray diffraction, whereas the study by transmission electron microscopy revealed that the catalyst is mainly constituted of nickel phosphide particles of relatively uniform size dispersed within the SBA-15 channels. Both Ni_2P/SBA-15 and a reference Ni/SBA-15 catalyst were tested for the hydrodeoxygenation of methyl oleate ($C_{17}H_{33}-COO-CH_3$) in a fixed-bed continuous flow reactor. This compound was used as a convenient surrogate of triglyceride molecules present in vegetable oils that following catalytic hydrotreating yields *n*-alkanes as the main products. In the whole range of pressure studied (3−40 bar) and for temperatures higher than 290 °C, both systems achieve more than 80% ester conversion at 20 h^{-1} WHSV, although the Ni/SBA-15 catalyst presents a slightly higher activity. Overall, higher pressure and lower temperature and space velocity favors the formation of C_{18} hydrocarbon, which is the preferred product in terms of carbon atom economy. Nevertheless, under all the assayed conditions, the *n*-C_{18}/*n*-C_{17} ratio was remarkably higher for Ni_2P/SBA-15 than for Ni/SBA-15 catalysts. On the basis of these results, it can be concluded that both deoxygenation and decarboxylation occur simultaneously over the Ni_2P catalyst, whereas decarboxylation and cracking are the prevailing processes over the Ni catalyst. Owing to these high yields of long-chain paraffins, Ni_2P/SBA-15 can be considered as a very promising catalyst for the production of green diesel.

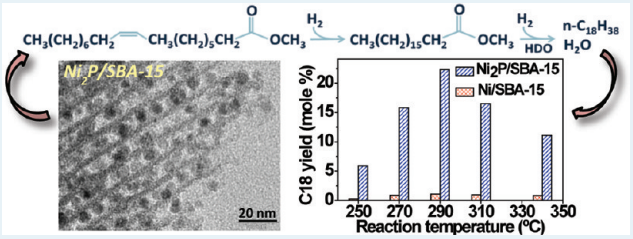

KEYWORDS: *hydrodeoxygenation, nickel phosphide, SBA-15, green diesel, biofuels, methyl oleate, triglycerides*

1. INTRODUCTION

Vegetable oils are suitable raw materials for the production of transportation fuels because their chemical structure is relatively akin to that of hydrocarbons in the distillation range of diesel fuel.[1] For that reason, in recent years, a considerable effort has been devoted to the production of biodiesel by transesterification of triglycerides with methanol, mainly under alkaline conditions.[1] The obtained fatty acid methyl esters (FAME) can be blended with conventional petrodiesel up to a maximum of 20% (B20 European biodiesel) and used in adapted engines.[2] However, FAME still has an O/C ratio similar to that of the original triglycerides, and consequently, these compounds still present lower calorific power, relatively high viscosity and cloud point, poor stability, and low volatility. Alternatively, oxygen can be removed from the biomass-derived molecules via a hydrotreating reaction named hydrodeoxygenation (HDO). This process can transform many oxygenated bioproducts into hydrocarbon molecules suitable as fuels.[3] In this way, triglycerides can be converted into what it is known as green or renewable diesel, composed mainly by hydrocarbons with a chain length in the $C_{14}-C_{20}$ range.[4−7]

Much research on reducing the O/C ratio of bioproducts by HDO has been performed using conventional supported metal sulfides such as Ni and Mo.[5−7] Although these catalysts are rather active for oxygen removal, regular addition to the feed of a sulfured agent is required to keep the activity for processing biomass feedstocks with low sulfur content. However, this operation is undesirable for both practical and environmental reasons. Noble metal catalysts such as Pt, Pd, or Re have also been used for HDO of nonedible vegetable oils, such as those obtained from jatropha crops,[5,8,9] but the high price of these active phases is detrimental for the production of cost-effective biofuels. In addition, although Pd/C catalyst is rather active for hydrotreating fatty acids such as caprylic or stearic, it favors the decarboxylation reaction route and, consequently, provides

Received: December 14, 2011
Revised: February 19, 2012
Published: February 24, 2012

higher selectivity toward C_{N-1} hydrocarbons (N is the number of carbons of the fatty acid).[5,9] However, considering carbon atom economy, C_N alkanes are the preferred products because they are formed by hydrogenation of the carbonyl group, and consequently, the reaction does not release CO_2, but H_2O. Although this process consumes more hydrogen, reducing CO_2 generation also avoids unwanted hydrogenation side reactions to yield methane. Therefore, the development of more efficient and selective catalysts for hydrodeoxygenation of vegetable oil into hydrocarbon products still constitutes a significant challenge, which will require a shift from traditional metal sulfide or precious metal catalysts to alternative active phases. In this way, it is known that transition metal phosphides (TMPs) show chemical properties similar to noble metals, and they are particularly active for hydrotreating reactions, especially in hydrodesulfurization.[10−15]

Recently, it has been also reported that transition metal phosphides are effective for oxygen removal from molecules present in bio-oils such as guaiacol,[16] 4-methylphenol,[17] or anisole.[18] Dispersion of metal phosphides on mesostructured supports could further enhance their hydrotreating performance, as reported for HDS dibenzothiophene and HDN of *o*-methyl aniline over Ni_2P supported on SBA-15 and KIT-6.[19] However, to our knowledge, these types of catalytic systems have not been applied to the HDO of biomass derived molecules. Within this context, we here compare the activity of nickel phosphide supported on SBA-15 with conventional Ni/SBA-15 catalyst for the HDO of methyl oleate, which has been selected as a convenient surrogate of triglyceride molecules of vegetable oils. The obtained results show that Ni_2P/SBA-15 presents a significantly higher selectivity and yield of C_{18} hydrocarbons than conventional Ni/SBA-15 catalyst under a wide range of conditions.

2. EXPERIMENTAL SECTION

2.1. Catalyst Preparation. For the synthesis of SBA-15, the structure-directing agent, Pluronic 123 (MW 5800, Aldrich), was dissolved in HCl solution at room temperature and then heated to 40 °C before adding tetraethylorthosilicate (TEOS, Aldrich), used as silica source. This mixture was stirred for 20 h at 40 °C and aged at 100 °C for 24 h under autogenous pressure. Thereafter, the solid product was recovered by filtration and dried overnight. The surfactant was removed by calcination at 550 °C for 5 h. The SBA-15-supported nickel phosphide, Ni_2P/SBA-15, (20 wt % Ni) was prepared by wet impregnation of aqueous solutions of nickel nitrate and ammonium phosphate (Aldrich) in a Ni/P molar ratio of 1:1, followed by drying and calcination at 500 °C, and subsequent temperature-programmed reduction (TPR) at 650 °C in H_2. For characterization purposes, this sample was further passivated for 6 h by soft oxidation in air according to the procedure described elsewhere to avoid the total oxidation of the active phases.[13] For comparison, 20 wt % Ni/SBA-15 with the same nickel loading was also prepared by a procedure similar to that of the supported nickel phosphides except for the final reduction temperature, which for this catalyst was 450 °C.

2.2. Catalyst Characterization and Testing. Elemental analysis was performed after microwave digestion of the samples in an ICP-AES Optima 7300 DV (Perking-Elmer) instrument. The nitrogen adsorption−desorption experiments were performed at 77 K on a Quadrasorb system (Quantachrome). XRD patterns of the catalysts were recorded with a Philips PW 3040/00 X'Pert MPD/MRD diffractometer using Cu Kα radiation operated at 45 kV and 40 mA. TEM images of the catalysts were taken using a Philips TECNAI 20T instrument, working at 200 kV and equipped with an EDX spectrometer for measuring X-ray energy dispersive spectra. The activity of the catalysts was studied in a fixed-bed reactor operated at a pressure ranging from 3 to 40 bar and at temperatures in the 250−340 °C range, with a feedstock containing methyl oleate (70%, Aldrich) in heptane (total ester content: 10 wt %). About 200 mg of catalyst pelletized, crushed and sieved with 40−60 mesh, and then mixed with silicon carbide was used in the assays. The hydrogen flow rate was 30 mL/min, and the organic phase was introduced at a rate of 6 $mL{\cdot}h^{-1}$, corresponding to a space velocity of 20.4 h^{-1} (WHSV), although for some experiments, the space velocity was increased up to 81.6 h^{-1}. Liquid samples collected at 1 h intervals were analyzed off-line by a gas chromatograph (Agilent, 7890A) equipped with a FID and two columns, HP-5 for paraffin analysis and HP-INNOWAX for ester analysis.

3. RESULTS AND DISCUSSION

3.1. Physicochemical Characterization of the Catalysts. As was mentioned above, to stabilize the reduced form of the catalysts, samples passivated were used for characterization. Textural properties of SBA-15 support and the catalysts were obtained from the N_2 adsorption−desorption isotherms, which are displayed in Figure 1. The values of the different parameters obtained from the isotherms are summarized in Table 1. All the samples possess type IV sorption isotherms (Figure 1a), typical of mesoporous ordered materials. The pore size distribution obtained by Barret−Joyner−Halenda (BJH) analysis of these curves shows no marked differences among the samples, which in all cases present a maximum centered at a diameter around 6.7 nm. However, from this analysis it is observed that the mesopore volume is more than 50% lower for Ni_2P/SBA-15 than for SBA-15, but in the case of Ni/SBA-15, the volume reduction is about 30%. Accordingly, both catalysts have lower BET (from the Brunauer, Emmett and Teller equation) specific surface areas (S_{BET}) than SBA-15, although this reduction is, again, significantly more marked for Ni_2P/SBA-15 (Table 1). This behavior is related to the accumulation of the active phase inside the SBA-15 channels, which is more extensive in the case of the nickel phosphide sample than for the Ni/SBA-15. This suggests that most Ni_2P particles, as well as some P_4/P_2 species formed during the reduction of the phosphate excess,[12] are mainly located inside the channel of the mesostructured silica. Similar results in terms of decreasing both surface area and pore volume on introducing nickel phosphide have been previously reported by Korányi et al.[19]

Figure 2a shows the low-angle X-ray diffraction patterns of SBA-15 and the passivated catalysts. Only the most intense characteristic peak of SBA-15 structure can be observed for both Ni_2P/SBA-15 and Ni/SBA-15. This fact indicates that the structural order of SBA-15 decreases for the supported catalysts, very likely due to the uneven distribution of active phase particles inside the pores. The high-angle X-ray diffraction patterns of SBA-15 and the passivated catalysts are displayed in Figure 2b. For SBA-15, the broad peak at around 22° is due to amorphous silica as usually found for these mesostructured materials, which consist of an ordered array of channels located between amorphous silica walls. The characteristic peaks of Ni_2P appearing at 40.6, 44.5, 47.2, and

dx.doi.org/10.1021/cs200659r | ACS Catal. 2012, 2, 592−598

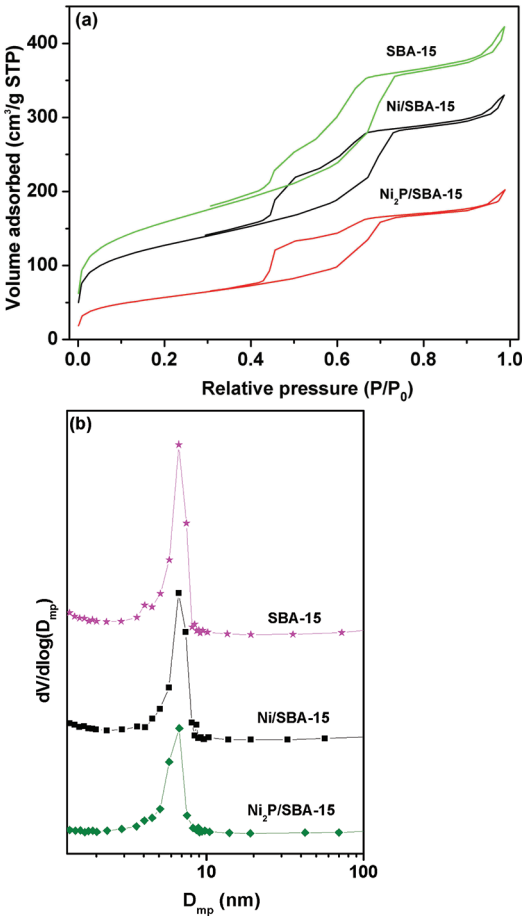

Figure 1. (a) N_2 sorption isotherms and (b) BJH pore size distribution of SBA-15 and the passivated catalysts.

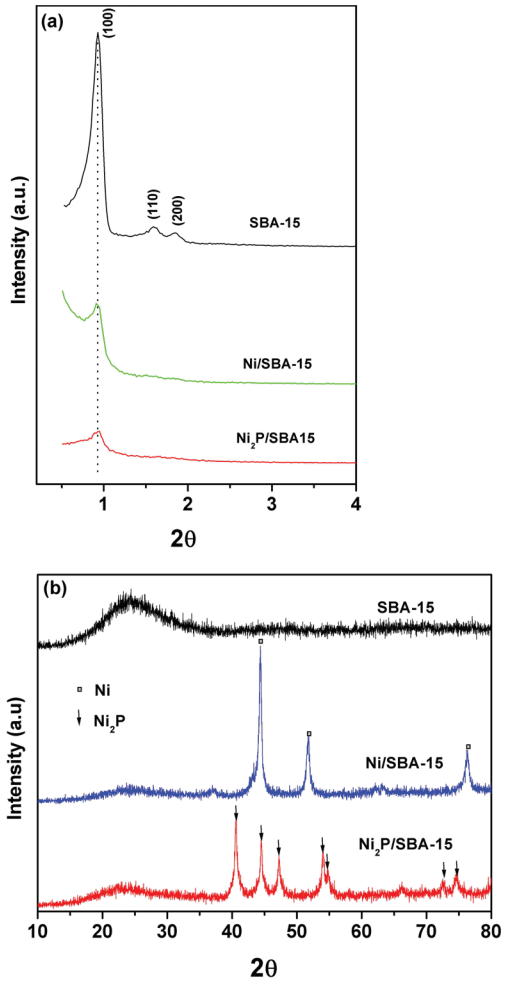

Figure 2. (a) Low and (b) wide-angle X-ray diffraction patterns of SBA-15 and the passivated catalysts.

54.0° are clearly shown, confirming the formation of this phase over the SBA-15 matrix (JCPDS 74-1385). The reflections at 44.3, 51.8, and 76.3° present in the Ni/SBA-15 pattern also confirm the existence of crystallites of metallic nickel (JCPDS 04-0850).

Figure 3 shows TEM images and TEM−EDX analysis results of the Ni_2P/SBA-15 sample. This study reveals that small Ni_2P particles with a rather homogeneous size distribution (average diameter < 7 nm) are well-dispersed within the mesopores of SBA-15 (Figure 3a). This indicates that SBA-15 is an excellent support for dispersing nickel phosphide because the mesopores stabilize nanoparticles size and provide good sintering resistance, even though this sample was prepared at 650 °C. In addition, a much lower proportion of larger Ni_2P particles with a diameter of ∼25 nm and a globular morphology are detected outside of SBA-15 channels.

TEM images of these large particles also show evidence of the passivation layer because a light gray band is observed in the external edge of Ni_2P with a thickness of ∼1.5 nm (Figure 3b). On the basis of the EDX analysis, the Ni/P mole ratio of the Ni_2P particle is determined to be close to the stoichiometric mole ratio of ∼Ni/P = 2. Figure 4 displays the TEM images and TEM−EDX analysis result of the Ni/SBA-15. The Ni crystallites are more prone to form aggregates than Ni_2P, and this fact leads to the formation of large Ni particles over the SBA-15 external surface. In addition, Ni particles present a rather wide size distribution (25−60 nm) and a more irregular morphology as compared with Ni_2P crystallites. These results are consistent with the N_2 adsorption isotherm of Ni/SBA-15, which shows that the porous structure is much less affected by the incorporation of the metal than in the case of nickel phosphide.

3.2. Catalytic Activity. Hydrogenation of the methyl oleate double bond under mild conditions yields methyl stearate,[20]

Table 1. Physicochemical Properties of the SBA-15 Support and the Ni-Containing Catalysts

samples	Ni content (wt %)	bulk composition	S_{BET} (m^2/g)	V_{meso} (cm^3/g)	V_{total}[a] (cm^3/g)	D_{mp}[b] (nm)
SBA-15			599	0.5	0.70	6.70
Ni/SBA-15	19.6	Ni	462	0.38	0.51	6.69
Ni_2P/SBA-15	18.8	$Ni_{1.97}P$	206	0.28	0.31	6.73

[a]Total pore volume calculated from the N_2 adsorption at relative pressure of 0.98. [b]Mesopore size calculated from the adsorption branch of the N_2 isotherm using the BJH method.

dx.doi.org/10.1021/cs200659r | ACS Catal. 2012, 2, 592−598

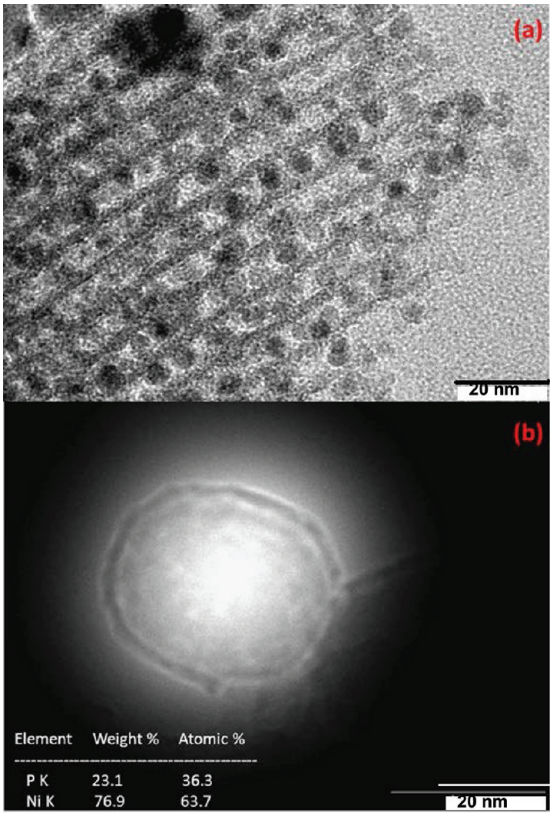

Figure 3. (a) TEM images and (b) TEM–EDX analyses of Ni_2P/SBA-15.

but this reaction, despite contributing to the conversion of this FAME, does not contribute to a decrease in the O/C ratio. On the contrary, removal of the ester group of the methyl oleate, either by decarboxylation to C_{17} alkanes or HDO to C_{18} paraffins, is a more relevant process for the upgrading of triglycerides.[6] Accordingly, to take into account exclusively deoxygenation reactions, total ester conversion is considered in this study. The evolution of this parameter is shown in Figure 5

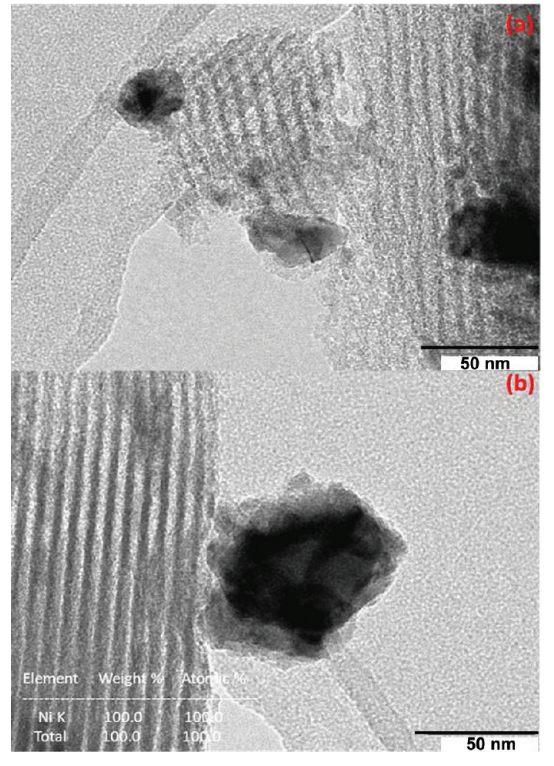

Figure 4. (a) TEM images and (b) TEM–EDX analyses of Ni/SBA-15.

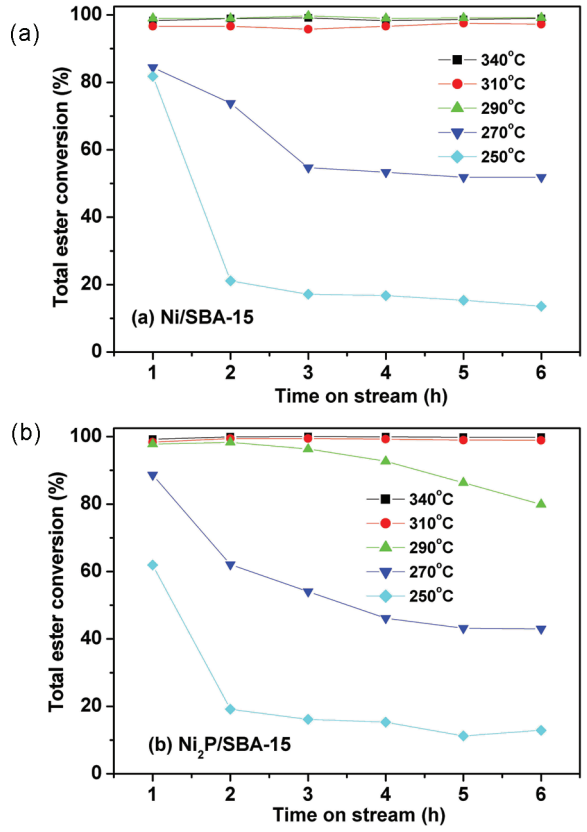

Figure 5. Variation of total ester conversion at different temperatures as a function of time on-stream over (a) Ni/SBA-15 and (b) Ni_2P/SBA-15 catalysts. Reaction conditions: 30 bar; WHSV = 20.4 h^{-1}; H_2/feedstock ratio = 300 $Nm^3 \cdot m^{-3}$.

as a function of time on stream over Ni_2P/SBA-15 and Ni/SBA-15 catalysts at temperatures in the 250–340 °C range and at 30 bar of pressure. Nearly complete conversion of esters is achieved over both catalysts at temperature higher than 290 °C. However, ester conversion quickly declines with decreasing temperature, and at 250 °C, it drops below 20%. In the whole range of temperatures, Ni/SBA-15 is slightly more active than Ni_2P/SBA-1%, although the activity of both catalysts for the conversion of methyl oleate approaches 16 μmol·mol $Ni^{-1} \cdot s^{-1}$ at the higher temperature of operation.

On the other hand, these catalysts initially show some deactivation at low reaction temperature, which is more progressive for Ni_2P/SBA-15. This fact is very likely related to the accumulation of byproduct of the reaction that can partially block the active sites. In this respect, thermogravimetric analysis coupled to mass spectrometry (TG–MS) of the Ni_2P/SBA-15 catalyst after reaction at 250 °C (see the Supporting Information (SI)) shows two events, one of which can be associated with the combustion of the reagents remaining on the surface that occurs simultaneously to the desorption of methyl oleate residues; the other can be related to the oxidation of more bulky molecules or coke. On the other

dx.doi.org/10.1021/cs200659r | ACS Catal. 2012, 2, 592–598

hand, Figure 6 displays ester conversion at 270 °C after 6 h on-stream for both catalysts as a function of the space velocity. As

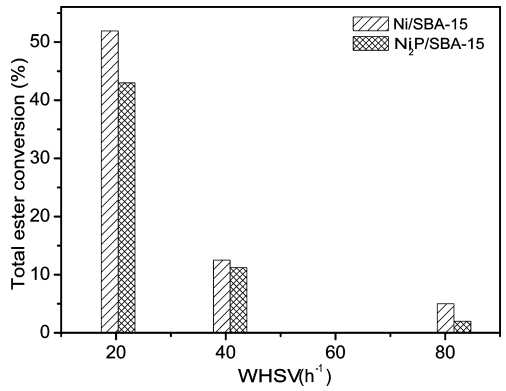

Figure 6. Variation of total ester conversion at 270 °C after 6 h on-stream as a function of the space velocity for Ni/SBA-15 and Ni_2P/SBA-15 catalysts. Reaction conditions: H_2/feedstock ratio = 300 $Nm^3 \cdot m^{-3}$.

expected, conversion drops with increasing space velocity, but in all cases, it remains slightly higher for Ni/SBA-15 than for Ni_2P/SBA-15.

Gas phase analysis reveals the formation of methane and minor amounts of CO and CO_2 in the outlet stream. These results suggest that methanation of CO_x is significant under these operation conditions. In the liquid phase, linear paraffins are the main products detected, but traces of methanol and free saturated fatty acids (mostly stearic) are detected in most of the catalytic runs. More specifically *n*-alkanes in the C_{15}−C_{18} range, which are formed from a feedstock composed mainly of C_{18} (80%) and C_{16} (9%) fatty acids, are the predominant products. In the case of the Ni/SBA-15 catalyst, C_{17} paraffin is produced in a higher proportion under all assayed conditions (Figure 7).

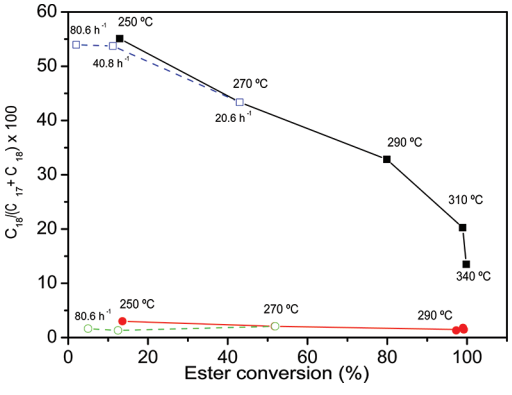

Figure 7. Evolution of the $C_{18}/(C_{17} + C_{18})$ ratio with conversion over Ni_2P/SBA-15 (squares) and Ni/SBA-15 catalysts (circles). The solid symbol corresponds to assays performed at different temperatures at WHSV = 20.4 h^{-1}, and the open symbol corresponds to catalytic runs performed at 270 °C at different space velocities. Other reaction conditions: 30 bar; H_2/feedstock ratio = 300; 6 h on-stream.

However, because it can be clearly understood in Figure 7, the selectivity to C_{18} *n*-alkanes is significantly higher for the Ni_2P/SBA-15 catalyst, particularly at lower temperatures and high space velocity, when conversion is lower than 15% and the $C_{18}/(C_{17} + C_{18})$ ratio approaches 0.55.

In contrast, for Ni/SBA-15, the $C_{18}/(C_{17} + C_{18})$ ratio remains lower than 0.03 and relatively constant with changing conversion. Taking into account the low conversion data (<10%) obtained at 270 °C with 81.6 h^{-1} space velocity, it can be concluded that the higher selectivity of Ni_2P/SBA-15% is not due to the operation conditions, but rather, it is an intrinsic characteristic of this catalyst. In terms of *n*-octadecane yield (see Figure 8), the maximum value (25%) is achieved for Ni_2P/

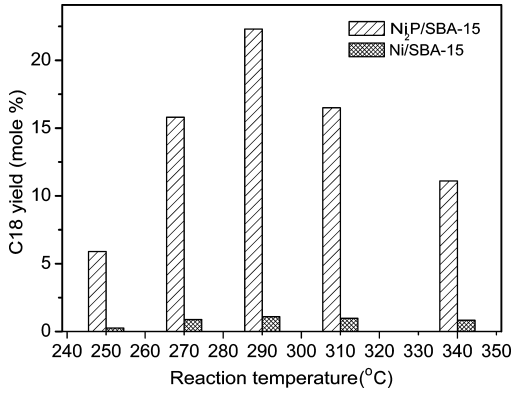

Figure 8. Variation the C_{18} yield with temperature over Ni_2P/SBA-15 and Ni/SBA-15 catalysts. Reaction conditions: 30 bar; WHSV = 20.4 h^{-1}; H_2/feedstock ratio = 300 $Nm^3 \cdot m^{-3}$.

SBA-15 at 290 °C; for Ni/SBA-15, it is lower than 2% at all the assayed temperatures. On the other hand, the decline in yield at temperatures higher than 290 °C for Ni_2P/SBA-15 can be attributed to the larger contribution of the decarboxylation processes.

A more detailed comparison of the differences in the product distribution over both nickel and nickel phosphide catalysts is displayed in Figure 9 for tests performed at 340 °C and 30 bar over 6 h. Considering that the FAME fed to the reactor contains about 80% C_{18} and 9% C_{16} fatty acids, it seems clear that Ni/SBA-15 induces extensive cracking, leading to a significant yield of alkanes in the C_9−C_{15} range, especially at higher temperatures. In contrast, cracking is not significant for

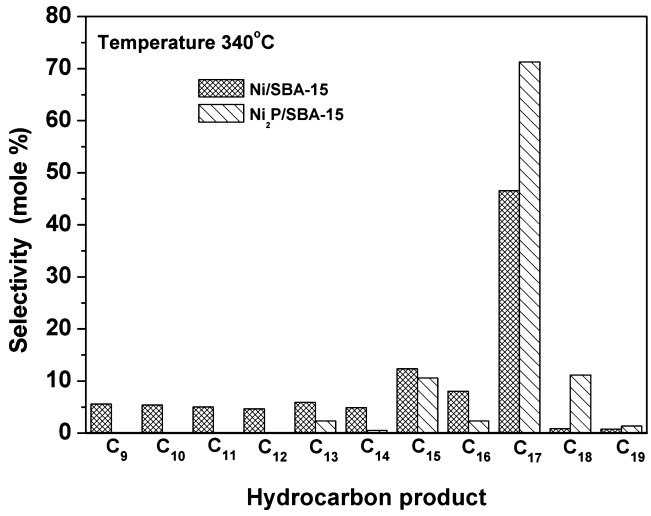

Figure 9. Comparison of the hydrocarbon product distribution over Ni_2P/SBA-15 and Ni/SBA-15 catalysts. Reaction conditions: 340 °C; 30 bar; WHSV = 20.4 h^{-1}; H_2/feedstock ratio = 300 N $m^3 \cdot m^{-3}$; time on-stream = 6 h.

dx.doi.org/10.1021/cs200659r | ACS Catal. 2012, 2, 592−598

the Ni_2P/SBA-15 catalysts under the conditions used in the present study, and this catalyst yields a rather narrow product distribution, which is basically constituted by the products of decarboxylation (C_{17} and minor amount of C_{15}) and deoxygenation (C_{18} and a minor amount of C_{16}). Consequently, Ni_2P/SBA-15 appears as a very promising alternative for green diesel production from vegetable oils.

The effect of H_2 pressure on the performance of the two catalysts was evaluated at 250 °C because at this temperature, a higher HDO selectivity is obtained. The results shown in Figure 10 indicate that FAME conversion after 6 h on-stream increases

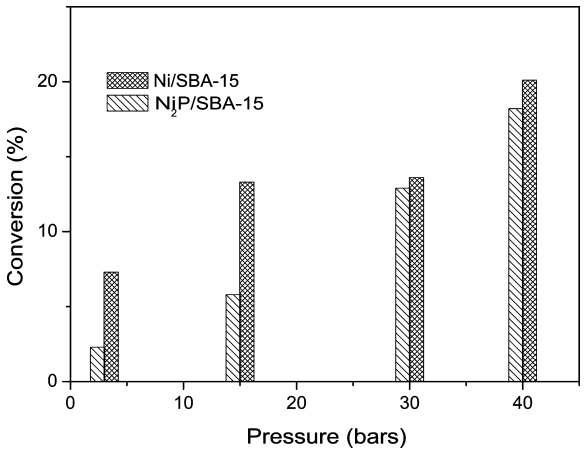

Figure 10. Variation of the total ester conversion after 6 h on-stream as a function of pressure for Ni/SBA-15 and Ni_2P/SBA-15 catalysts. Reaction conditions: 250 °C; WHSV = 20.4 h^{-1}; H_2/feedstock ratio = 300 N $m^3 \cdot m^{-3}$; time on stream = 6 h.

almost linearly with pressure. As in the case of the temperature variation, the Ni/SBA-15 catalyst is slightly more active than Ni_2P/SBA-15 at all the investigated pressures. On the other hand, Figure 11 displays the variation of the $C_{18}/(C_{17} + C_{18})$

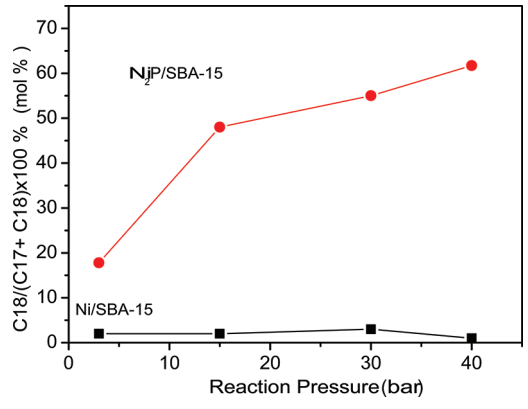

Figure 11. Evolution of the $C_{18}/(C_{17} + C_{18})$ ratio with H_2 pressure over Ni_2P/SBA-15 and Ni/SBA-15 catalysts. Reaction conditions: 250 °C; WHSV = 20.4 h^{-1}; H_2/feedstock ratio = 300 $Nm^3 \cdot m^{-3}$; time on stream = 6 h.

ratio with pressure for both catalysts. Selectivity of Ni/SBA-15 for HDO remains quite low and rather insensitive to the hydrogen pressure, suggesting that on this catalyst, the contribution of the hydrodeoxygenation route to hydrocarbon formation is very limited.

In contrast, for Ni_2P/SBA-15, a sharp increment in $C_{18}/(C_{17} + C_{18})$ ratio is observed at higher hydrogen pressures. More specifically, a remarkable enhancement of the selectivity is observed when the pressure rises from 3 to 15 bar, and a more progressive increase in the production of C_{18} alkanes is appreciated up to 40 bar. As can be understood from Figure 12,

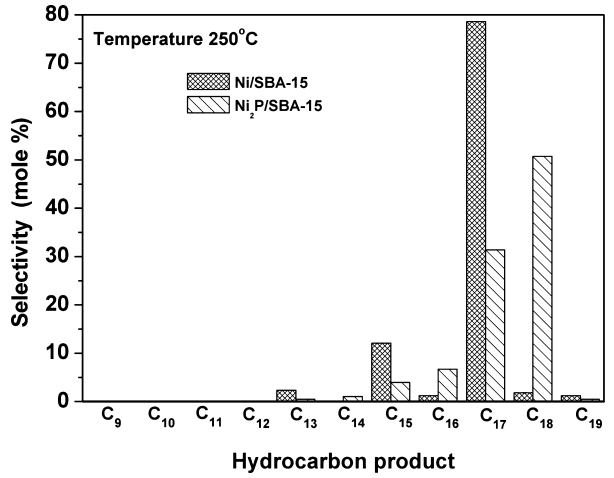

Figure 12. Comparison of the hydrocarbon product distribution over Ni_2P/SBA-15 and Ni/SBA-15 catalysts. Reaction conditions: 250 °C; 40 bar; WHSV = 20.4 h^{-1}; H_2/feedstock ratio = 300 $Nm^3 \cdot m^{-3}$; time on stream = 6 h.

at 250 °C and 40 bar, cracking is rather limited and Ni/SBA-15 yields basically decarboxylation products, whereas under these conditions, HDO is greatly promoted for Ni_2P/SBA-15. Therefore, considering the economy of the process, operating at moderate pressures (20−30 bar) can provide an adequate HDO yield with lower hydrogen consumption.

On the basis of these results, it can be concluded that the transformation of FAME molecules takes place according to rather different routes, depending on the chemical nature of the active phase. Thus, both deoxygenation and decarboxylation occur simultaneously over the Ni_2P catalyst, and decarboxylation and cracking are the prevailing processes over the Ni catalyst. Previous works have suggested that the presence of 4-fold coordinated tetrahedral Ni sites, denoted as Ni(i), and 5-fold coordinated square pyramidal, Ni(ii), over the Ni_2P crystallite surface are responsible for its unique selectivity.[14] More specifically, the Ni(ii) sites can be associated with the superior hydrogenation ability of Ni_2P, leading to the enhanced selectivity toward C_{18} *n*-alkanes.

On the other hand, it is suggested that the Ni (i) site may be involved in the activation of the CH_3OOC-$C_{17}H_{35}$ bond, leading to the decarboxylation route. Considering that the proportion of these types of active sites varies with the Ni_2P particle size,[14,15] a finer control of crystallite diameter may provide a way to further tune the selectivity of this catalyst. It will be studied in future works.

4. CONCLUSIONS

Pure silica SBA-15 is an excellent support for Ni_2P dispersion in the form of spherical and uniform nanoparticles, which are incorporated inside the ordered mesopores of this material. Hydrotreating of methyl oleate over the Ni_2P/SBA-15 catalyst promotes decarboxylation and hydrodeoxygenation reactions, yielding C_{17} and C_{18} hydrocarbons, respectively. In contrast,

dx.doi.org/10.1021/cs200659r | ACS Catal. 2012, 2, 592−598

Ni/SBA-15 favors cracking reactions in addition to decarboxylation, giving rise to a broader hydrocarbon distribution. Adjusting the reaction conditions allows the extension of hydrodeoxygenation versus decarboxylation to be controlled in the case of the Ni_2P/SBA-15 catalyst. Thus, lowering the reaction temperature and space velocity and increasing the pressure leads to HDO selectivity around 60% for Ni_2P/SBA-15, whereas this parameter remained at a very low value for Ni/SBA-15. Therefore, Ni_2P/SBA-15 can be considered a very promising catalyst for green diesel production from vegetable oils because of its high efficiency in the removal of oxygen by a combination of decarboxylation and hydrodeoxygenation pathways, the latter becoming predominant at moderate temperatures.

■ ASSOCIATED CONTENT

Supporting Information

TG-MS data of the Ni_2P/SBA-15 catalyst after reaction is available in the Supporting Information file. This material is available free of charge via the Internet at http://pubs.acs.org/.

■ AUTHOR INFORMATION

Corresponding Author

*E-mail: david.serrano @imdea.org.

Notes

The authors declare no competing financial interest.

■ ACKNOWLEDGMENTS

This study has received financial support from the RESTOENE program funded by Consejería de Educación, Comunidad de Madrid and LIGNOCATUP from the Spanish Ministry of Science and Innovation (ENE2011-29643-C02-01). Y.X.Y. and V.P.O. are grateful for financial support from, respectively, the AMAROUT (European Comission) and Ramón y Cajal (MICINN) programs.

■ REFERENCES

(1) Behr, A.; Westfechtel, A.; Pérez Gomes, J. *Chem. Eng. Technol.* **2008**, *31*, 700−714.
(2) Knothe, G. *Prog. Energy Combust.* **2010**, *36*, 364−376.
(3) Tushar, P.; Vispute, H.; Zhang, A.; Sanna, R.; Xiao, G.; Huber, W. *Science* **2010**, *330*, 1222−1227.
(4) Kubickova, I.; Snare, M.; Eranen, K.; Maki-Arvela, P.; Murzin, P. *Catal. Today* **2005**, *106*, 197−200.
(5) Boda, L.; Onyestya, G.; Solt, H.; Valyon, J.; Thernesz, A. *Appl. Catal., A* **2010**, *374*, 158−169.
(6) Kubicka, D.; Kaluz, L. *Appl. Catal., A* **2010**, *372*, 199−208.
(7) Kubicka, D; Horácek., J. *Appl. Catal., A* **2011**, *394*, 9−17.
(8) Ping, E. W.; Pierson, J.; Wallace, R.; Miller, J. T.; Fuller, T. F.; Jones, C. W. *Appl. Catal., A* **2011**, *396*, 85−90.
(9) Murata, K.; Liu, Y.; Inaba, M.; Takahara, I. *Energy Fuels* **2010**, *24*, 2404−2409.
(10) Kim, H. Y.; Ma, X. L.; Song, C. S. *Energy Fuels* **2005**, *19*, 353−364.
(11) Yang, S. F.; Liang, C. H.; Prins, R. *J. Catal.* **2006**, *237*, 118−130.
(12) Gaudette, A. F.; Burns, A. W.; Hayes, J. R.; Smith, M. C.; Bowker, R. H.; Seda, T.; Bussell, M. E. *J. Catal.* **2010**, *272*, 18−27.
(13) Sun, F. X.; Wu, W. C.; Wu, Z. L.; Guo, J.; Wei, Z. B.; Jiang, Z. X.; Tian, F. P.; Li, C. *J. Catal.* **2004**, *228*, 298−310.
(14) Oyama, S. T. *J. Catal.* **2008**, *258*, 393−400.
(15) Oyama, S. T.; Gott, T.; Zhao, H. Y.; Lee, Y. K. *Catal. Today* **2009**, *143*, 94−107.
(16) Zhao, H. Y.; Li, D.; Bui, P.; Oyama, S. T. *Appl. Catal., A* **2011**, *391*, 305−310.
(17) Victoria, M.; Whiffen, L.; Smith, K. *Energy Fuels* **2010**, *24*, 4728−4737.
(18) Li, K.; Wang, R.; Chen, J. *Energy Fuels* **2011**, *25*, 854−863.
(19) Koranyi, T. I.; Coumans, A. E.; Hensen, J. M.; Ryoo, R.; Kim, H. S.; Pfeifer, E.; Kasztovszky, Z. *Appl. Catal., A* **2009**, *365*, 48−54.
(20) Deliya, V.; Simakova, I. L.; Ravasio, N.; Psaro, R. *Appl. Catal., A* **2009**, *357*, 170−177.